A brief introduction to fusion and stellarators

Issra Ali (email), on behalf of UTNEA

Feb 2026

The purpose of this document is to build, from the ground up, a necessary background on the physics of stellarators in order to understand what you are doing when performing stellarator optimization. We highly recommend that you read this before the competition. The salient points will be stated in the introductory lectures of the competition, and hearing these concepts after having read of them yourself will help you learn.

1 Nuclear energy

Featured on kitschy posters, t-shirts, and most unfortunately, tattoos around the world is the mass-energy equivalence, a result from Einstein's theory of special relativity:

$$E = mc^2 \tag{1}$$

This equation implies that a ball at the top of a ramp, for example, is lighter than a ball on the ground. For the same reason, every atomic nucleus, save hydrogen, is lighter than the sum of its constituent nucleons. The bound nucleons are deeper in the "well" of potential energy associated with their bonds than free nucleons are. The depth of this well is called the nuclear binding energy, which varies for different isotopes; the degree to which the constituent nucleons are lighter varies accordingly. The binding energy per nucleon is plotted for various isotopes in fig. 1.

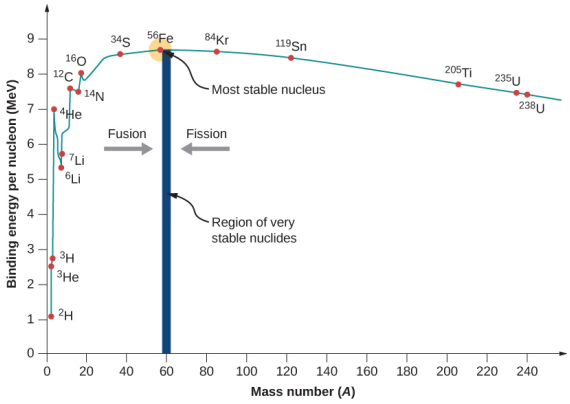

Figure 1: A diagram of the nuclear binding energy of some notable isotopes, from [1].

It is the goal of nuclear fusion and fission alike to take advantage of these differences in binding energy per nucleon: when nuclei with more binding energy per nucleon; i.e. lighter nucleons, are formed from those with less binding energy per nucleon, the "mass deficit" is released as kinetic energy of the reactants. Fusion involves combining nuclei to make a nucleus with lighter nucleons, whereas fission involves splitting a nucleus into products with lighter nucleons. The amount of energy per fusion reaction of deuterium (Hydrogen-2) and tritium (Hydrogen-3), the most common fusion fuels, is 17.6 MeV. This is a ridiculously large amount: just a kilogram of deuterium-tritium fuel possesses the same amount of energy as the chemical energy in 2.6 million gallons of gasoline.

2 Fusion reactors

At the nuclear scale, causing a fusion reaction entails bringing nuclei close enough together that the strong interaction causes them to combine into a single nucleus. This is no easy task, since the Coulomb repulsion between the nuclei dominates the strong force at any internuclear separation of more than a few femtometers. The temperatures at which the particles have sufficient energy to reach these distances during collisions correspond, at feasible densities, to plasmas.

It is the job of a fusion reactor to make fusion reactions likely. A figure of merit for fusion reactors known as the Lawson criterion can be devised, which is instructive to explain the conditions required to maximize the rate of fusion:

$$nT\tau_E \geq 3 \cdot 10^{21} \text{ keV} \frac{\text{s}}{\text{m}^3} \tag{2}$$

where n is density, which must be increased so that reactions occur more frequently, T is temperature, which must be increased so the reactants collide with sufficient energy to overcome the Coulomb repulsion between them, and τ_E is the energy confinement time, which describes how well the reactor is keeping heat in the plasma. The confinement time is computed as $\tau_E = \frac{W}{P_{out}}$, the quotient of the energy contained within the plasma W and the rate of energy loss from the reactor P_{out}. The number on the right-hand side of (2) is the value that must be exceeded if the machine is to produce more energy output than input.

2.1 Magnetic confinement

Magnetic confinement fusion devices seek to maximize temperature and confinement time by heating the fuel to a plasma and imposing a strong magnetic field to contain it. The way in which a magnetic field can confine a plasma can be understood by considering the motion of a particle with charge q and velocity $\mathbf{v}$ in a uniform magnetic field $\mathbf{B} = B\hat{\mathbf{e}}_z$:

$$m\dot{\mathbf{v}} = q\mathbf{v} \times \mathbf{B} \tag{3}$$

where $q\mathbf{v} \times \mathbf{B}$ is the Lorentz force. Because the Lorentz force acts only normal to $\mathbf{v}$, the acceleration produced by it is purely centripetal. The particle therefore undergoes circular gyration perpendicular to the magnetic field, and is not accelerating parallel to the field. Recognizing this, the following can be written:

$$m\frac{v_\perp^2}{\rho} = qv_\perp B \tag{4}$$

Accordingly, the radius of the orbit ("gyroradius") is given as:

$$\rho_c = \frac{mv_\perp}{qB} \tag{5}$$

and the "gyrofrequency", the rate at which the particles orbit the field lines, is computed:

$$\Omega = \frac{v_\perp}{\rho} = \frac{qB}{m} \tag{6}$$

Therefore, charged particles are free to move along magnetic field lines, but have no net displacement in the direction perpendicular to the field.

To leverage this fact to confine a plasma, the field lines can be wrapped into a torus, permitting particles to travel along them indefinitely. Doing so, however, necessarily creates gradients in the magnetic field strength

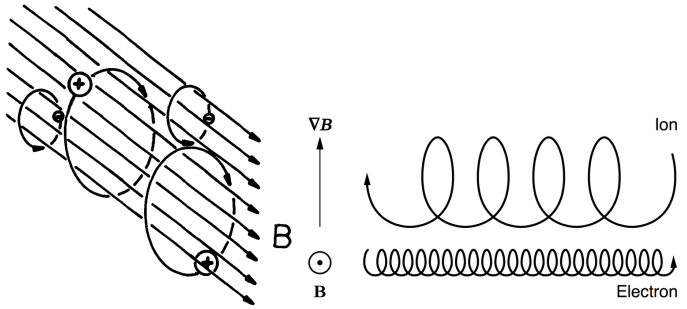

Figure 2: Left: charged particle motion in a magnetic field. Notice that electrons and ions rotate in different directions (as expected from (6)), from [2]. Right: cross particle drift due to a gradient in the magnetic field strength. Note that this picture is looking directly down a magnetic field line; the reason that this drift occurs is that the gyro-radius is larger in regions of lower field than in regions of higher field, as is clear in (5)

that lead to cross-field drift effects, which ruin confinement [3] (see fig. 2 left, and caption for explanation). These must be countered by ensuring that field lines pass through both high-field (inboard side) and low-field strength (outboard side) regions of the torus; that is, the field lines must twist. They must have a poloidal (the short way around, ϑ in fig. 4) component, as opposed to being purely toroidal (the long way around, φ in fig. 4) [4]. The number of times that a field line makes a poloidal transit per toroidal transit is called the rotational transform ι.

There are two ways to produce this poloidal component: by running a current through the plasma, as done in tokamaks, or by 3D geometric shaping, as done in stellarators (see fig. 3). Broadly speaking, the tokamak is easier to fabricate due to its axisymmetry, but driving its current makes the reactor susceptible to instabilities when it is operating. The stellarator is exempt from these instabilities, but is generally more difficult to manufacture.

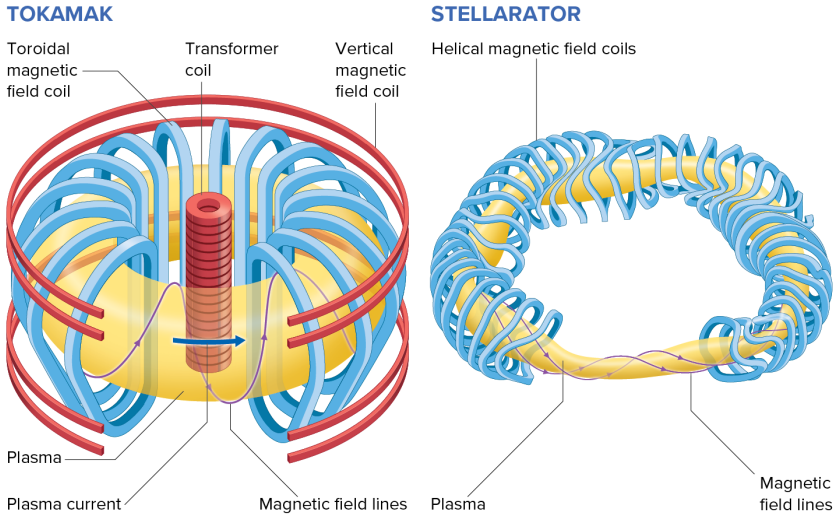

Figure 3: A tokamak (left) and a stellarator (right). The poloidal field component of the tokamak is created by inducing a current in the plasma by essentially using it as the secondary of a transformer coil, while the poloidal field component in the stellarator is created purely geometrically. Graphics from [5]

At this point, it is worth reflecting on the goal of maximizing the triple product from the particular context of stellarators. There are a variety of mechanisms by which a magnetic confinement fusion reactor can lose energy and particles (and thereby have a low confinement time and triple product). The most important

include heat conduction and particle diffusion from the plasma ("classical transport"), neoclassical (see § 4.1) and turbulent transport, as well as radiative emissions (bremsstrahlung, cyclotron emission, electron line emissions, etc).

Interestingly, in stellarators, many of these transport avenues are tied to the geometry of the plasma: for example, neoclassical particle transport in stellarators can be reduced even below tokamak levels by shaping the magnetic field in certain ways § 4.2. Put concisely, **geometry determines confinement quality**, and the field of stellarator optimization seeks to leverage this fact to design reactors with superior performance.

3 The basics of magnetic confinement physics

3.1 Plasmas

A plasma is an ionized gas. Plasmas can be created in a number of ways, for example, by subjecting a gas to a large potential difference, collisional or radiative ionization (collision with particles or photons), or photoabsorption.

A key attribute of a plasma that is very relevant to transport in stellarators is the collisionality ν_{ab}, which roughly corresponds with the frequency of collisions between particles of species a and b in a gas; however, the actual meaning of it is more subtle. Because the particles that constitute a plasma are charged, they interact at long ranges via the Coulomb force, and can be deflected at small angles in addition to single collisions that cause a large change in direction. The collisionality, precisely speaking, is the inverse of τ_{ab}, which is the average time it takes for a particle of species a to be deflected a total angle of 90 degrees by particles of species b. The collisionality scales inversely with temperature as: $\nu \sim T^{-3/2}$, which seems to defy intuition from gas dynamics, in which the collision rate between particles scales with temperature. However, there is simple physical reasoning for this: at higher kinetic energies (higher T), the Coulomb force has less time to do work on particles.

Like a gas, a kinetic description (i.e. the Boltzmann equation) is the most accurate and general for a plasma; in fact, kinetic descriptions remain necessary to capture many phenomena that are of interest for fusion reactors. However, simpler fluid models capture many of the important dynamics and are used as a basis for the reactor design.

3.2 Magnetohydrodynamic equilibria

The simplest useful model of a stellarator or tokamak plasma is the magnetohydrodynamic equilibrium equation (also called the magnetohydrostatic equation),

$$\mathbf{J} \times \mathbf{B} = \frac{1}{\mu_0}(\nabla \times \mathbf{B}) \times \mathbf{B} = \nabla p \tag{7}$$

which may be viewed as the Navier-Stokes momentum equation in the limit $\frac{\partial}{\partial t} \to 0, \mathbf{v} \to 0$, with the Lorentz force $\mathbf{J} \times \mathbf{B}$ replacing the body-force/gravity term. Of course, the magnetic field must obey Gauss' law $\nabla \cdot \boldsymbol{B} = 0$ as always.

A useful intuitive picture may be immediately extracted from (7): $\mathbf{B}, \mathbf{J}$ lie on nested toroidal surfaces of constant pressure. This can be seen by noting that $\mathbf{B} \cdot \nabla p = 0, \mathbf{J} \cdot \nabla p = 0$, and applying the hairy ball

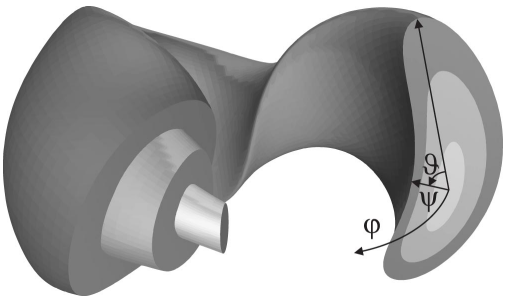

Figure 4: A diagram showing the nested pressure/flux surface structure of an MHD equilibrium, along with labels for local toroidal coordinates, from [4]

theorem, which states that a non-vanishing vector field can only be everywhere tangent to a surface if the surface is topologically toroidal (see fig. 4). The pressure surfaces are typically called "flux surfaces", because the magnetic flux in the φ direction enclosed within any pressure isosurface is constant with respect to the variable φ (precisely because $\mathbf{B} \cdot \nabla p = 0$).

An extremely useful family of curvilinear coordinate systems, called "magnetic coordinates" or "flux coordinates", are used to describe the dynamics in an MHD equilibrium. Magnetic coordinates are aligned to the magnetic field, such that field lines appear straight. Typically, these are written as $(\rho, \vartheta, \varphi)$, where ρ is the radial coordinate or "flux surface label", and ϑ, φ are conventionally called the poloidal and toroidal magnetic angles (though they of course, do not actually have to be poloidal and toroidal). The curve $\rho = 0$ is called the magnetic axis. The rotational transform ι can be computed as $\frac{d\vartheta}{d\varphi}$.

The MHD equilibrium model is useful for various calculations and is, moreover, the starting point for more detailed simulations that capture physics outside of the MHD model, such as neoclassical and turbulent transport, resistive effects, etc. Crucially, as will become clear later, geometrical properties that correspond to improved neoclassical or turbulent confinement can be obtained immediately from the results of an MHD solve, making it the workhorse model for stellarator optimization.

Analytical solutions of the model exist only for simple geometries, particularly for basic tokamak configurations. There are ways to construct solutions with more general geometries analytically using a method called the "near axis expansion", which involves an asymptotic expansion in the inverse aspect ratio (e.g. a/R, the quotient of minor and major radius) around a provided magnetic axis shape. More generally, however, and for plasmas relevant for fusion devices, numerical methods are required.

3.2.1 Solution of the MHD equilibrium equation with `DESC`

The MHD equilibrium problem is most commonly solved with a spectral method; one code that implements such a method is the `DESC` code [6]. The residual of (7) is computed as a function of the field components in magnetic coordinates. In `DESC`, the magnetic coordinates are themselves a function of real-space Cartesian coordinates; the problem of solving the PDE is converted into a problem of *choosing a mapping from magnetic coordinates to real-space coordinates* that minimizes the force error. A Fourier series is used as an ansatz for the mapping from real-space coordinates as a function of the magnetic coordinates:

$$\left.\begin{aligned} R(\rho,\theta,\varphi) &= \sum R_{lmn}(\rho)\mathcal{Z}_l^m(\rho,\theta)\cos(m\theta - N_{fp}n\varphi) \\ Z(\rho,\theta,\varphi) &= \sum Z_{lmn}(\rho)\mathcal{Z}_l^m(\rho,\theta)\sin(m\theta - N_{fp}n\varphi) \end{aligned}\right\} \tag{8}$$

where ρ is the radial coordinate (or flux surface label), θ is the modified poloidal magnetic angle[1], φ is the toroidal magnetic angle (which is taken to be the polar azimuthal angle), and $\mathcal{Z}_l^m$ are Zernike polynomials (a set of orthogonal polynomials). Here, m ranges from $0, \ldots, M$ and n from $-N, \ldots, 0, \ldots N$. N_{fp} is the number of field periods, i.e. degree of discrete toroidal rotational symmetry of the stellarator § 3.2.2. Therefore, we can write the problem that `DESC` solves as:

$$\min_{R_{lmn}, Z_{lmn}} ||\boldsymbol{J} \times \boldsymbol{B} - \nabla p|| \tag{9}$$

A solution of the above problem is determined by:

1. The shape of the outermost flux surface (a.k.a. the Last Closed Flux Surface or LCFS) i.e., $R_{mn}(\rho = 1), Z_{mn}(\rho = 1)$,
2. Two radial profiles (often the pressure and toroidal current profiles)

Often times in stellarator optimization, we begin by optimizing a *vaccum field*, i.e. we set the pressure and current profiles to zero, and our solution is completely determined by the geometry of the boundary. In free-boundary mode, the field is computed from the coils, which are separated from the portion of the domain with finite plasma pressure by a vacuum.

3.2.2 Stellarator symmetry and field periodicity

Note in (8) that a cosine-only Fourier series is used for the R coordinate, and a sine-only series for the Z coordinate. This is an imposed symmetry called "stellarator symmetry" that serves the purpose of shrinking the design space and making machines more easily engineerable. More precisely, stellarator symmetry is the constraint:

$$R(\rho, \theta, \varphi) = R(\rho, -\theta, -\varphi), Z(\rho, \theta, \varphi) = -Z(\rho, -\theta, -\varphi) \tag{10}$$

The integer factor N_{fp} serves a similar purpose: it is the number of "field periods", or the number of times the same section of plasma is repeated toroidally (see fig. 5)

4 Stellarator optimization

The link between the geometry of a stellarator and the physics/confinement quality raises the question: does there exist a best possible stellarator design? This is the question that the field of stellarator optimization seeks to answer.

In practice, many stellarator optimization researchers have adopted the **two-stage paradigm**: in stage-one optimization, fixed-boundary optimization is performed (i.e., determining the best possible LCFS). In the second stage, a separate optimization loop is used to find coils that can match the magnetic field on the outermost flux surface; i.e. coils that minimize $\boldsymbol{B} \cdot \hat{\boldsymbol{n}}$ on the LCFS. This is done because the physics of the

[1]For the sake of not clouding the physical intuition of the cursory reader, I have told you a small lie by omission. The modified θ used in 8 is different than the ϑ used when I introduced magnetic coordinates; this is not a mistake! The ϑ is a true magnetic coordinate, which uniquely forms magnetic coordinates (i.e. coordinates where the field lines appear straight) when φ is taken as the typical polar azimuthal angle. θ is a modified version of ϑ used for purely computational reasons: θ is chosen such that the representation is more "spectrally dense"; i.e., you need fewer coefficients for the Fourier series in R, Z to converge. The relationship between θ and ϑ is: $\vartheta = \theta + \lambda(\rho, \theta, \varphi)$. We use a Fourier-Zernike basis as an ansatz for λ and determine it during our equilibrium solve, so there really should be a third row in 8 with $\lambda(\rho, \theta, \varphi) = \sum \lambda_{lmn}(\rho) \mathcal{Z}_l^m(\rho, \theta) \sin(m\theta - N_{fp} n \varphi)$

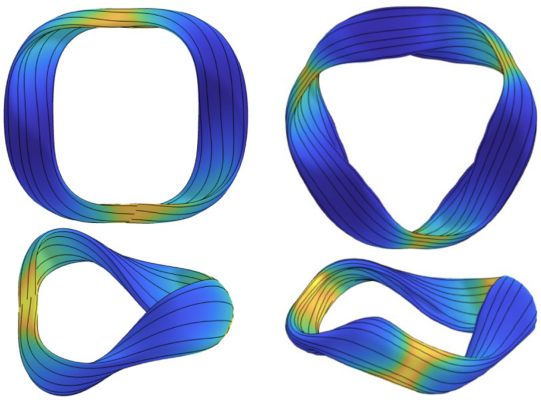

Figure 5: A $N_{fp} = 2$ (left) and a $N_{fp} = 3$ (right) configuration, from [7]

reactor essentially depend only on the LCFS, and there exist many coil sets that can produce the exact same LCFS. Engineering concerns about the coils are relegated to stage-two optimization, while concerns about the physics of the reactor are the focus of stage-one optimization.

Stage one optimization can be posed as:

$$\min_{R^b_{mn}, Z^b_{mn}} f(\boldsymbol{B}, p), \tag{11}$$

$$\text{such that } \boldsymbol{J} \times \boldsymbol{B} = \nabla p \text{ in } \Omega, \tag{12}$$

$$\boldsymbol{B} \cdot \boldsymbol{n}(\boldsymbol{x}) = 0 \text{ on } \partial\Omega \tag{13}$$

where R^b_{mn}, Z^b_{mn} are the Fourier coefficients describing the shape of the stellarator boundary. Stage two optimization can be posed as:

$$\min_{\boldsymbol{x}_{\text{coils}}} \left[\left(\boldsymbol{B}(\boldsymbol{x}_{\text{coils}}) \cdot \hat{\boldsymbol{n}}(R^b_{mn}, Z^b_{mn}) \right) |_{\rho=1} + f_{\text{engineering}}(\boldsymbol{x}_{\text{coils}}) \right] \tag{14}$$

where $\boldsymbol{x}_{\text{coils}}$ are the degrees of freedom parametrization the coils (often described with splines or a Fourier series, see `DESC` docs for more details) and $f_{\text{engineering}}(\boldsymbol{x}_{\text{coils}})$ is a penalty to make the coils simpler to manufacture, which may include metrics such as curvature (lower curvature is better) and coil length (less total coil length is cheaper).

A massive success story of stellarator optimization is the development of the neoclassically optimized stellarator. Historically, stellarators were outshone by their axisymmetric tokamak cousins because they suffered far greater neoclassical transport (see § 4.1), to the point that some were convinced that a stellarator reactor would be impossible! The word "optimized" in the term "optimized stellarator" initially referred to optimization to reduce neoclassical transport; an objective whose experimental achievement by the reactor Wendelstein 7-X propelled the stellarator to finally produce plasmas competitive with tokamak H-mode discharges (the most performant plasmas in tokamaks) [8]. The following introduces neoclassical transport and describes the "quasi-symmetric stellarator", which is a type of neoclassically optimized stellarator.

4.1 The basics of neoclassical transport

Neoclassical transport arises due to the non-uniformity of the magnetic field strength that necessarily exists in toroidal fusion devices. At centre stage in the theory of neoclassical transport are "trapped orbits".

In a highly magnetized plasma, in which the gyroradius is small and the gyrofrequency large, the motion of a particle can be simplified by looking at its "guiding centre", i.e., its motion with the gyration about magnetic field lines averaged. In making this average, it is assumed that the magnetic moment $\mu = \frac{mv_\perp^2}{2B}$, is conserved. The total energy can then be written:

$$E = \frac{1}{2}mv_\parallel^2 + \mu B \tag{15}$$

Combined, conservation of energy and conservation of μ imply that a particle with energy E cannot enter a location with magnetic field strength $B > B_{max} = \frac{E}{\mu}$, because its parallel velocity must switch signs in order for it to conserve energy; that is, the particle is trapped in a region with $B < B_{max}$. The particles bounce off these regions of high field, undergoing periodic motion called trapped or banana orbits, as pictured in fig. 6.

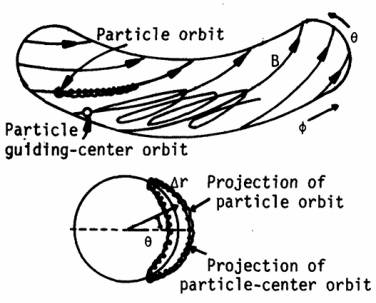

Figure 6: A diagram illustrating the actual motion of a particle in the magnetic field (top, filled dot), the guiding centre motion of a bouncing orbit (top, unfilled dot), and the projection of the trapped orbit in the poloidal plane (bottom), from which the trapped orbits earned the nickname "banana orbits", from [2]

In general, a trapped particle will accrue some radial displacement throughout a trapped orbit [4] due to forces related to curvature, gradients of the magnetic field within a flux surface, etc. The speed at which a trapped particle drifts radially is called v_d. Even with no collisions, a trapped particle would eventually leave the plasma in a general magnetic field. This effect is exacerbated into an unfavourable transport scaling in collisional plasmas.

Banana orbits occur at a frequency called the "bounce frequency"; the crux of neoclassical transport is that different transport phenomena occur depending on the relationship between the collisionality of the plasma and the bounce frequency. When the collisionality is much lower than the bounce frequency (which occurs at fusion-relevant temperatures), the plasma enters the $1/\nu$ neoclassical transport regime (see fig. 7). In this region, the neoclassical diffusion coefficient for species a is given:

$$D \sim \frac{\epsilon_{\text{eff}}^{3/2} v_d^2}{\nu_a} \tag{16}$$

where ν_a is the collisionality, v_d is the radial drift speed of the guiding centre of trapped particles, and ϵ_{eff} is a factor that is related to the fraction of particles in the plasma that are trapped. The basic reasoning for this is that particles in trapped orbits are undergoing random walks of length $\Delta x = v_d \cdot \Delta t$ in the time $\Delta t = \nu^{-1}$, and the diffusion coefficient is (as typical for a random walk) estimated as $\frac{(\Delta x)^2}{\Delta t}$. This regime of

transport is prohibitively bad for a magnetic fusion reactor.

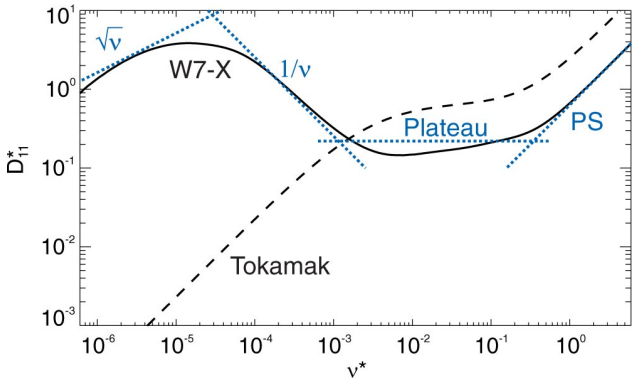

Figure 7: A diagram displaying the variation in the neoclassical diffusion coefficient D^*_{11} for tokamaks and stellarators as a function of collisionality ν^*, which is the typical collisionality ν normalized to make this a fair comparison. Note that there is no $1/\nu$ regime for tokamaks, while there is one for stellarators.

Tokamaks have zero v_d; therefore, they confine collisionless particles and do not experience the deadly $1/\nu$ regime. The same cannot be said for stellarators in general. The reason for this ultimately comes down to the fact that tokamaks are axisymmetric. The most beautiful way of seeing this (and the way most instructive in demonstrating how one may fix this problem in stellarators) uses Noether's theorem, which states that symmetries in dynamical systems correspond to conserved quantities.

The dynamics of a charged particle in the magnetic field of a tokamak do not depend on the toroidal coordinate. More precisely, the gyro-averaged Lagrangian of a particle in a tokamak can be written in cylindrical coordinates as:

$$\mathcal{L}(R, \varphi, Z, \dot{R}, \dot{\varphi}, \dot{Z}) = \frac{m}{2}\dot{\mathbf{R}}^2 + q\mathbf{A}\cdot\dot{\mathbf{R}} - q\varphi \tag{17}$$

where $\mathbf{A}$ is the magnetic vector potential, $\dot{\mathbf{R}}$ is the velocity vector, and φ is the electric potential (note that $\mathbf{A}, \varphi$ contain all the same information as $\mathbf{B}, \mathbf{E}$ and are related as $\nabla \times \mathbf{A} = \mathbf{B}, \mathbf{E} = -\nabla\varphi$; they are just more convenient in this context). For a tokamak, $\mathbf{A}$ and φ are independent of the polar angle φ, and so the corresponding canonical momentum p_φ is conserved, as evident from the Euler-Lagrange equation in φ:

$$\frac{d}{dt}p_\varphi = \frac{d}{dt}\left(\frac{\partial\mathcal{L}}{\partial\dot{\varphi}}\right) = \frac{\partial\mathcal{L}}{\partial\varphi} = 0 \tag{18}$$

In an abstract sense, this is already enough to conclude that trapped orbits are confined in a tokamak: including the magnetic moment and the energy, there are three conserved quantities. The particle only has three degrees of freedom (the three spatial dimensions in which it can move); the motion must be confined to some submanifold of the phase space that keeps these constants of motion the same.

More directly, it can be shown that p_φ is indeed only dependent on the radial coordinate ρ, meaning that its conservation corresponds to particles remaining a fixed radial distance and that there is no net radial drift velocity v_d.

4.2 Quasisymmetric stellarators

Building on the intuition for why tokamaks have low neoclassical transport, one can design a stellarator with low neoclassical transport by engineering a symmetry into the field; this is called **"quasisymmetry"**.

A Lagrangian similar to the one in (17) can be written in a certain type of magnetic coordinates called Boozer coordinates $(\rho_B, \vartheta_B, \varphi_B)$ for a stellarator. The only term in this Lagrangian that is dependent on the poloidal or toroidal magnetic coordinates is a term involving B, the magnetic field strength. Therefore, a symmetry of the magnetic field strength in this coordinate system is a symmetry of the Lagrangian. For a full treatment, see [4].

Quasisymmetric (QS) stellarators are those whose fields have strength contours with a symmetry in some linear combination of the toroidal and poloidal Boozer coordinates; that is, $B = B(\rho, \eta)$ with $\eta = M\vartheta_B - N\varphi_B$. Just as in a tokamak, these devices have a conserved canonical momentum corresponding to the variable η. The case $M = 1, N = 0$ is called quasi-axisymmetric (QA), and cases $M = 1, N \neq 0$ are called quasi-helically symmetric (QH).

Fields with near-perfect QS have been achieved in the last three years through shape optimization [9]; they are plotted in fig. 8. They have been shown to have comparable neoclassical confinement properties to tokamaks [10].

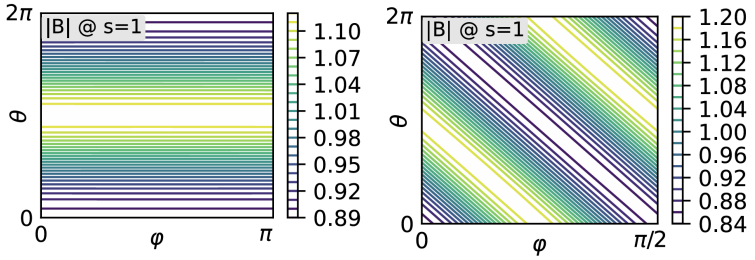

Figure 8: (Left) A plot of the magnetic field strength contours of a (nearly perfect) optimized quasi-axisymmetric field in Boozer coordinates, with $B = B(\rho_B, \varphi_B)$; (Right) A (nearly perfect) quasi-helically symmetric field, with $B = B(\rho_B, \vartheta_B - \varphi_B)$ (from [9])

Previous results were much less quasisymmetric:

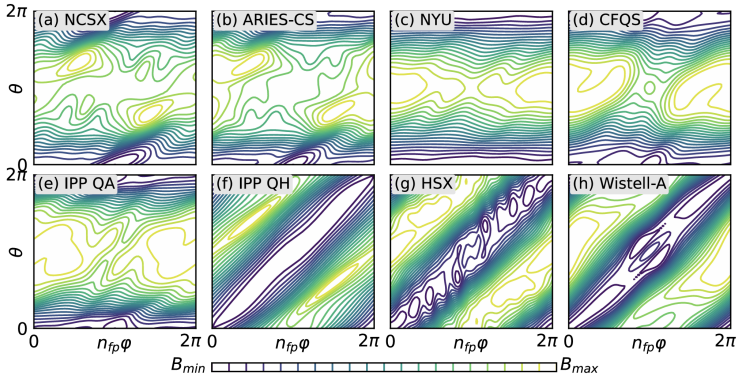

Figure 9: An assortment of Boozer plots of QA and QH fields from the stellarator literature, prior to [9] (from [9])

It is worth noting that is a sufficient, but not necessary, condition for omnigeneity. The necessary condition (that there is no net radial excursion over a bounce orbit) is called omnigeneity, and there are other ways, besides quasisymmetry, that it can be achieved. The reactor Wendelstein 7-X in Greifswald, Germany, is an example of an omnigenous reactor of the "quasi-isodynamic" type. Constructing more generally omnigenous fields is out of the scope of this competition.

4.3 Beyond neoclassical optimization

Now that neoclassical optimization in stellarators has more or less been "solved", the prevailing white whale in the field is the achievement of turbulent transport optimization (which is also the prevailing source of heat loss in tokamaks). Work has already been done to link stellarator geometry to turbulent transport [7, 11]; however, the field is still highly active.

5 Conclusion

We hope that this introduction has provided some useful background on stellarator optimization. Please feel free to reach out to me (issra.ali@mail.utoronto.ca)if you have any questions!

References

[1] *10.3: Nuclear Binding Energy*, en, Nov. 2016.

[2] T. J. Dolan, in *Fusion research*, edited by T. J. Dolan (Pergamon, 1982), pp. 151–167.

[3] L.-M. Imbert-Gerard, E. J. Paul, and A. M. Wright, (2019).

[4] P. Helander, Reports on Progress in Physics **77**, 087001 (2014).

[5] M. M. Waldrop, en, 10.1146/knowable-110123-1 (2023).

[6] D. Panici, R. Conlin, D. Dudt, K. Unalmis, and E. Kolemen, Journal of Plasma Physics **89**, 955890303 (2023).

[7] A. G. Goodman, P. Xanthopoulos, G. G. Plunk, H. Smith, C. Nührenberg, C. D. Beidler, S. A. Henneberg, G. Roberg-Clark, M. Drevlak, and P. Helander, en, PRX Energy **3**, 023010 (2024).

[8] S. Bannmann, 30th IAEA Fusion Conference (2025).

[9] M. Landreman and E. Paul, en, Physical Review Letters **128**, 035001 (2022).

[10] M. Landreman, S. Buller, and M. Drevlak, Physics of Plasmas **29**, 082501 (2022).

[11] M. Landreman, J. Y. Choi, C. Alves, P. Balaprakash, R. M. Churchill, R. Conlin, and G. Roberg-Clark, (2025).